Research Article ISSN 2767-3901

International Journal of Theoretical & Computational Physics

Concerning Built-In Potential of a Radial Asymmetrically Doped *P-N* Heterojunction in Core-Shell Nanowire

Vitalii L. Borblik

Department of Kinetic Phenomena and Polaritonics, V.Lashkarev Institute of Semiconductor Physics, Kyiv, Ukraine.

***Correspondence author**
Vitalii L. Borblik,
Department of Kinetic Phenomena and Polaritonics, V.Lashkarev Institute of Semiconductor Physics, Kyiv, Ukraine.

Submitted: 9 Dec 2025; **Accepted:** 13 Dec 2025; **Published:** 5 Jan 2026

Citation: Borblik, V. L. (2026). Concerning Built-In Potential of a Radial Asymmetrically Doped *p-n* Heterojunction in Core-Shell Nanowire. *I J T C Physics, 7*(1):1-6. DOI : https://doi.org/10.47485/2767-3901.1068

Abstract

This article investigates theoretically electronic properties of radial type 1 p-n heterojunction in core-shell nanowire when doping level of the wide-gap layer is significantly higher than that of the narrow-gap one. The investigation takes into account contribution of excess free minority carriers into space charge of the narrow-gap part of the junction. By example of strongly asymmetric p^+- n heterojunction, it is shown that contribution of free minority carriers (as distinct from contribution of free majority ones) results in increase (rather than decrease) in both width of space charge region and built-in potential of the junction. This is important for electronics of photovoltaic devices. Value of the effect depends on p^+- n junction radius.

Keywords: Built-In Potential, Core-Shell Nanowire, Depletion Width, Energy Band Structure, Radial *P-N* Heterojunction, Space Charge.

Introduction

Currently semiconductor nanowires are used mostly in the form of multilayer structures in which material and/or doping type changes either in radial or axial direction. In particular, nanowires with p-n junctions have found broad and numerous applications as photo detectors (Costas et al., 2020), photovoltaic devices (Zhang & Liu, 2019), (Goktas et al., 2018), light emitting (Nami et al., 2018) and laser (Hua et al., 2009) diodes, tunnel diodes (Darbandi, et al., 2015) and bipolar transistors (Liborius et al., 2020). Numerous investigations have shown that radial core-shell nanowires have certain advances compared with axial ones because shell structure of nanowires provides, in particularly, passivation of their internal layers.

Unlike traditional electronics (microelectronics) where semiconductor structures are planar objects, the core-shell nanowires have cylindrical geometry that changes radically their electronic properties. In particular, in radial p-n junctions, depletion width in the core increases with decreasing junction radius, and depletion width in the shell, vice versa, decreases (Borblik, 2017; Borblik, 2018a). Wherein if in homojunctions, this influences only on position of the depletion region, then in heterojunctions, energy band structure are rebuilding, because change of the partial depletion widths results in change of relative contributions from different materials to the total depletion width. Furthermore, electronic properties of core-shell nanowires depend on sequence order of the layers relatively nanowire center (Borblik, 2018b; Borblik, 2024).

When considering p-n hetero junctions of 1st type, there are two possible configurations of composite materials (Figure 1): narrow-gap core/wide-gap shell (a) or, vice versa, wide-gap core/narrow-gap shell (b).

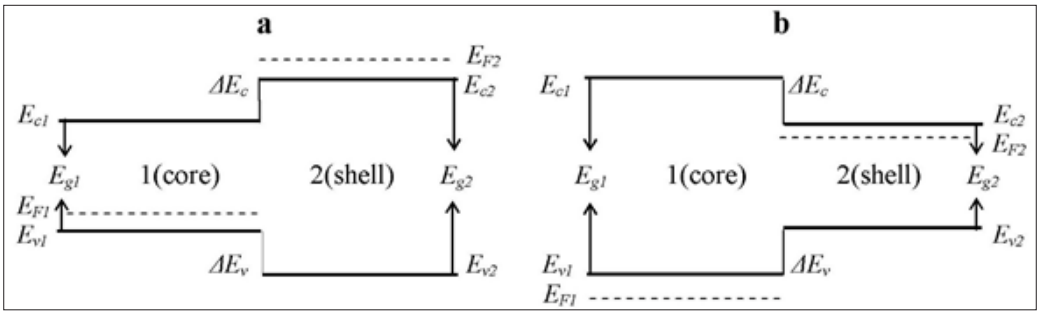

Figure 1: Possible energy band arrangement for type I *p-n* heterojunction; here E_{c1} and E_{c2} are bottoms of the conductivity bands, E_{v1} and E_{v2} are tops of the valence bands, ΔE_c and ΔE_2 are the energy bands discontinuities, E_{g1} and E_{g2} are the energy gaps, E_{F1} and E_{F2} are the Fermi levels.

If doping level of the wide-gap material is lower than that of the narrow-gap material, then in configuration (a), electrons transferred to narrow-gap part of the junction recombine with some part of holes; the rest of holes can diffuse into the n-part of the junction. In a similar way, in configuration (b), holes, transferred from wide-gap part of the junction to narrow-gap part, recombine with some part of electrons; the rest of electrons can diffuse into the *p*-part of the junction. Under these conditions, there are no free current carriers in proximity of metallurgical boundary of the junction. Space charge is created approximately by ionized impurities only (depletion approximation).

Depletion approximation turns out strict absolutely if doping levels are equal; then all current carriers transferred from the wide-gap parts to the narrow-gap ones recombine completely and space charge in the junction is created exclusively by ionized impurities. But if doping level of the wide-gap material is higher than that of the narrow-gap material, the latter acquires excess amount of free carriers which give contribution to space charge density in narrow-gap parts of the junction comparable with (and even much more than) contribution of ionized impurities. Below namely this case is considered theoretically.

Theory

We consider here radial p^+- n hetero junction in configuration (b) (Figure 2). In this figure, r_p is boundary of space charge region in the core, r_n is boundary of space charge region in the shell, and r_o is the *p*-*n* heterojunction radius.

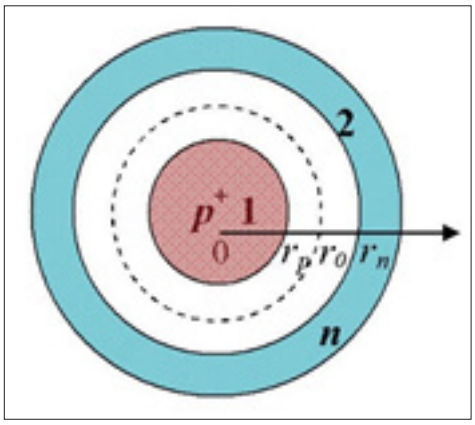

Figure 2: Schematic view of a radial p^+- n heterojunction.

Starting equations of the task are the Poisson's equation for two regions:

$$\frac{1}{r}\frac{d}{dr}\left(r\frac{d}{dr}V_l\right)=\frac{q}{\varepsilon_1}N_{A1}, r_p \le r \le r_0, \quad (1a)$$

$$\frac{1}{r}\frac{d}{dr}\left(r\frac{d}{dr}V_r\right)=-\frac{q}{\varepsilon_2}\left(N_{D2}+p_{ex}\exp\left(\frac{qV_r}{kT}\right)\right), r_0 \le r \le r_n. \quad (1b)$$

where V_l, V_r is electrostatic potential left and right relative r_o, q is electron charge, ε_1, ε_2 are dielectric constants of the materials, N_{A1} and N_{D2} are acceptor and donor concentrations, respectively, $p_{ex}=N_{A1}-N_{D2}$ is excess concentration of free holes in the narrow-gap shell, is the Boltzman's constant, T is absolute temperature.

In depletion approximation, i.e. without of term $p_{ex}\exp\left(\frac{qV_r}{kT}\right)$, solution of Eq. 1 is given by two transcendent equations for r_p and r_n which have to be solved jointly:

$$N_{A1}\left(r_0^2-r_p^2\right)=N_{D2}\left(r_n^2-r_0^2\right) \quad (2)$$

$$\frac{qN_{A1}}{2\varepsilon_1}\left(\frac{r_0^2-r_p^2}{2}+r_p^2\ln\frac{r_p}{r_0}\right)+\frac{qN_{D2}}{2\varepsilon_2}\left(\frac{r_0^2-r_n^2}{2}+r_n^2\ln\frac{r_n}{r_0}\right)=V_{bi}. \quad (3)$$

All the rest quantities are expressed through them. Built-in potential V_{bi} is determined by ionized impurities only in standard way.

Taking into account in Eq. 1b the contribution of free carriers we have non-linier equation of the 2nd order.

$$\frac{d^2V_r}{dr^2}+\frac{1}{r}\frac{dV_r}{dr}=a+b\exp\left(\frac{qV_r}{kT}\right) \quad (4)$$

where $a=-qN_{D2}/\varepsilon_2$, $b=-qp_{ex}/\varepsilon_2$. We reduce this equation to the system of differential equations of the 1st order

$$\frac{dV_r}{dr}\equiv\frac{dy_1}{dr}=y_2 \quad (5)$$

$$\frac{dy_2}{dr}+\frac{y_2}{r}=a+b\exp\left(\frac{qy_1}{kT}\right). \quad (6)$$

At the boundary condition $y_2(r_n)=0$ (electric field at edge of space charge region equals to zero) we obtain

$$y_2(r)=-\frac{1}{r}\left\{\int_r^{r_n}\left[a+b\exp\left(qy_1(r')/kT\right)\right]r'dr'\right\} \quad (7)$$

Then expression for electrostatic potential at boundary condition $y_1(r_n)=V_{bi}^{new}$ is

$$V_r(r)\equiv y_1(r)=\int_r^{r_n}\frac{dr'}{r'}\int_{r'}^{r_n}\left[a+b\exp\left(qy_1(r'')/kT\right)\right]r''dr''+V_{bi}^{new} \quad (8)$$

where V_{bi}^{new} contains contribution given by free holes.

Solution of Eq. 1a which satisfies boundary conditions $V_l(r_p)=0$, $\frac{dV_l}{dr}(r_p)=0$ is

$$V_l(r)=\frac{qN_{A1}}{2\varepsilon_1}\left[\frac{r^2-r_p^2}{2}+r_p^2\ln\left(\frac{r_p}{r}\right)\right] \quad (9)$$

Use of conditions of continuity of electrostatic induction and potential at interface r_0 allows us to calculate parameters r_p and r_n solving Eqs. 10-11 jointly

$$\varepsilon_1\frac{dV_l}{dr}(r_0)\equiv\frac{qN_{A1}}{2}\frac{r_0^2-r_p^2}{r_0}=-\frac{\varepsilon_2}{r_0}\left\{\int_{r_0}^{r_n}\left[a+b\exp\left(qy_1(r')/kT\right)\right]r'dr'\right\} \quad (10)$$

$$\frac{qN_{A1}}{2\varepsilon_1}\left[\frac{r_0^2-r_p^2}{2}+r_p^2\ln\left(\frac{r_p}{r_0}\right)\right]=\int_{r_0}^{r_n}\frac{dr'}{r'}\int_{r'}^{r_n}\left[a+b\exp\left(qy_1(r'')/kT\right)\right]r''dr''+V_{bi}^{new}. \quad (11)$$

Knowing general character of solution for potential (from the depletion approximation) it is not difficult by means of variation of r_p , r_n and V_{bi}^{new}, to pick up numerically $y_1(r)$ which satisfies Eq. 8 with as high accuracy as you like.

Results of the Numerical Calculations

For numerical calculations, hetero-pair GaAs/Ge was chosen as the closest to model of ideal heterojunction in view of close lattice constants. Parameters of both materials are taken from book of (Sze & Ng, 2006). Solutions of Eq. 8 obtained by means of above mentioned procedure at two values of acceptor concentration $N_{A1} = 2{\cdot}10^{18}$ and $5{\cdot}10^{18}$ cm^{-3} and donor concentration $N_{D2} = 10^{17}$ cm^{-3} (at the interface radius equal to 500 nm) are presented in Figure 3. Results of the depletion approximation are shown as well by dash lines.

It is seen from the figure that radial thickness of space charge region $w = r_n - r_p$ (as well as value of built-in potential) significantly increase at accounting of contribution of free carriers, in comparison with the depletion approximation.

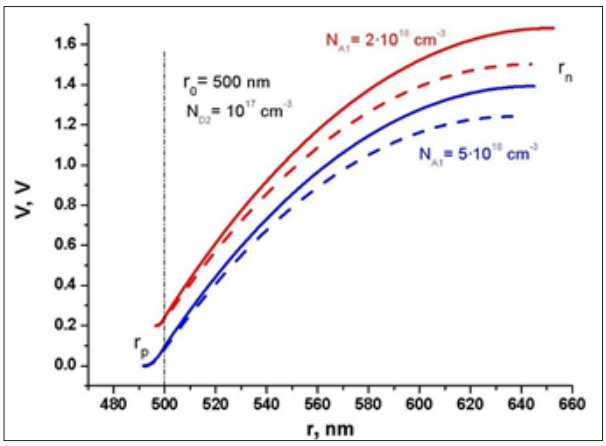

Figure 3: Graphs of solution of Eq. 8 with discrepancy between trial (i.e. located under integral) and obtained (after integration) solutions less than 0.1 %.

It is well known that taking into account contribution of *majority* carriers to space charge of *p-n* junction gives decreasing in its depletion width and built-in potential (Sze & Ng, 2006). As it follows from our results, taking into account contribution of *minority* carriers results, vice versa, in increasing in dimension of space charge region and built-in potential of *p-n* heterojunction.

Effect depends on junction radius. Behavior of electrostatic potential at interface radius of 500 nm (black), 100 nm (blue) and 40 nm (red) is presented in Figure 4 .

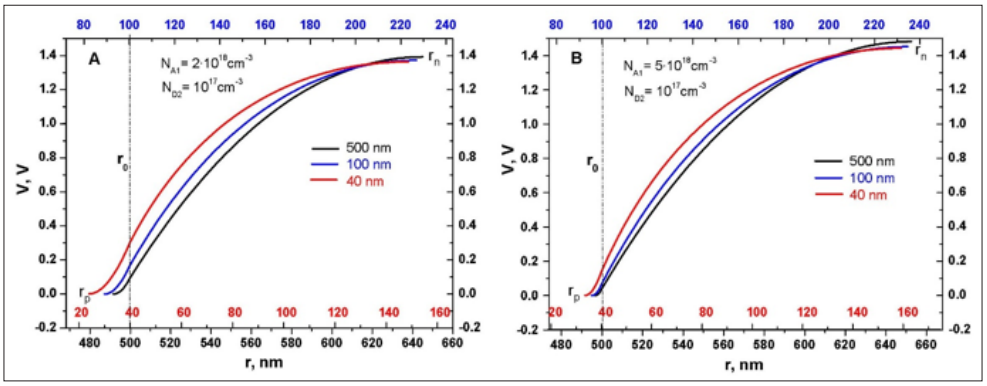

Figure 4: Radial distribution of electrostatic potential in the space charge region;
(A) – $N_{A1} = 2{\cdot}10^{18}$ cm^{-3}, (B) - $N_{A1} = 5{\cdot}10^{18}$ cm^{-3}.

From these distributions, explicit dependencies for total radial thickness of space charge region w and built-in potential V_{bi}^{new} on interface radius follow as presented in Figure 5 (in comparison with the depletion approximation results represented by dash lines).

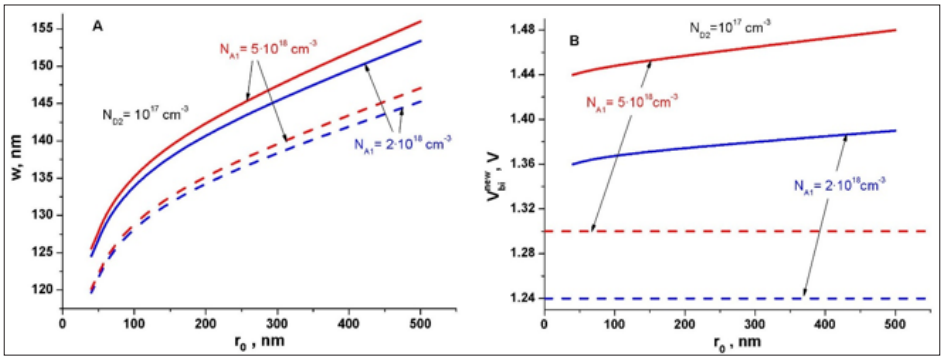

Figure 5: Dependencies of (A) total space charge region thickness of the heterojunction and (B) built-in potential on interface radius r_0 .

These dependencies demonstrate brightly role of curvature of the junction: at chosen doping levels, decreasing of the junction radius results in decreasing of large thickness of space charge region in the shell at insignificant increasing small thickness of space charge region in the core; so the total space charge region decreases. It should be noted that in the case of planar p^+-n junction (that corresponds to large value of r_o), considered effect is particularly significant.

Behavior of built-in potential V_{bi}^{new} with junction radius is qualitatively analogous. And its value is particularly large in "planar" case and falls with decreasing of the interface radius.

Figure 6 shows corresponding radial distributions of holes concentration in the space charge region at interface radius of 500 nm (black color), 100 nm (blue color) and 40 nm (red color). It corresponds completely to radial distribution of potential. At higher doping level of the core, the built-in potential is, as a whole, higher, and the holes concentration reaches lower values.

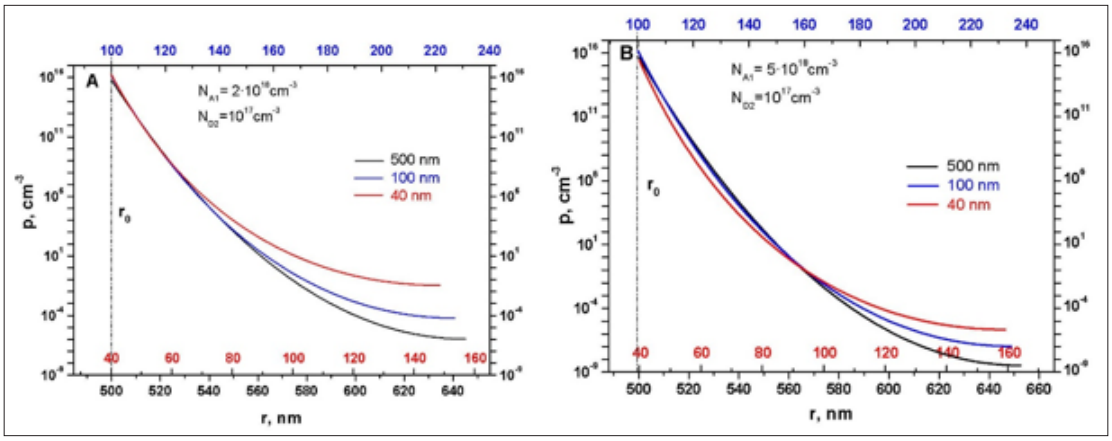

Figure 6: Radial distribution of holes concentration in space charge region;
(A) $N_{A1} = 2 \cdot 10^{18}$ **cm**$^{-3}$**, (B) -** $N_{A1} = 5 \cdot 10^{18}$ **cm**$^{-3}$**.**

It is of interest also to build energy band structure of the p^+-GaAs/n-Ge heterojunction. The energy band discontinuities ΔE_c and ΔE_v needed for this, are known with great scatter. We use values $\Delta E_c = 0.11$ eV and $\Delta E_v = 0.65$ eV which are common for two independent papers (Riben & Feucht, 1966) and (Donnelly & Milnes, 1967). Figure 7 demonstrates the calculation results at large interface radius (500 nm) showing comparison between the correct solution of the Poisson's equation and the depletion approximation. It is obvious that the correct solution noticeably increases heterobarrier.

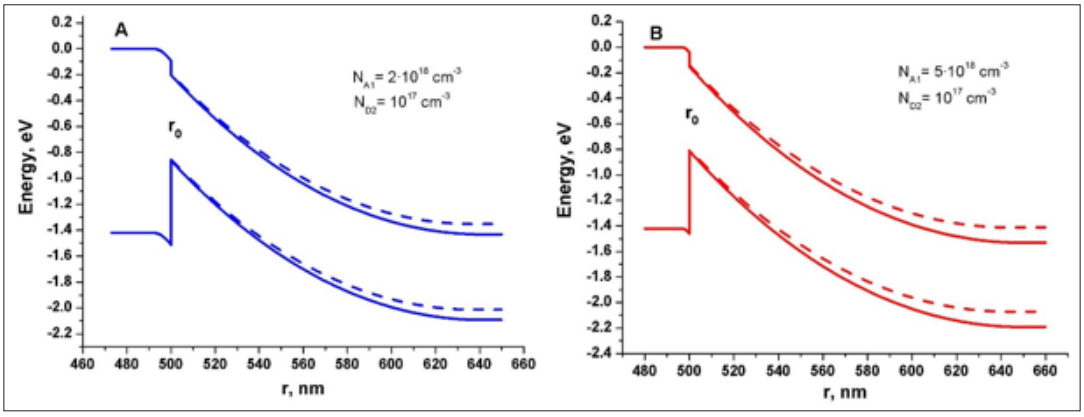

Figure 7: Energy band structure of the p^+-GaAs/n-Ge heterojunction at acceptor concentration of (A) $2 \cdot 10^{18}$ cm^{-3} and (B) $5 \cdot 10^{18}$ cm^{-3} in comparison with depletion approximation results (dash curves); interface radius equals to 500 nm

Figure 8 presents comparison of energy band structures of p^+-GaAs/n-Ge heterojunction at two interface radiuses - large (500 nm) and small (40 nm). Transfer from large radius to small one is accompanying by significant going down of the heterobarrier.

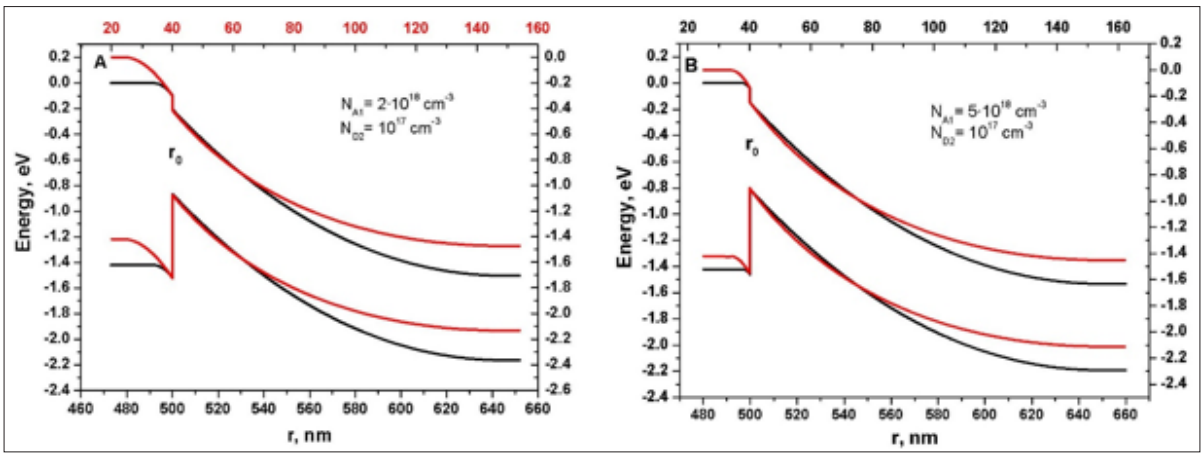

Figure 8: Energy band structure of the p^+-GaAs/n-Ge heterojunction at interface radiuses of 500 (black) and 40 (red) nm; the acceptor concentration is (A) $2 \cdot 10^{18}$ cm^{-3} and (B) $5 \cdot 10^{18}$ cm^{-3}.

Discussion

Correct solution of the Poisson's equation with taking into account contribution of free (in given case - *minority*) carriers results in significant change of the calculations results. Cylindrical geometry of nanowire imparts to these results yet dependence on *p-n* junction radius. Fundamental results concerning built-in voltage of the junction and dimension of its space charge region determine all other peculiarities of electronic properties of the heterojunction (character of spatial distribution of free carriers, value of heterobarrier).

From practical point of view, right doping of layers of *p-n* heterojunction of the 1st type, namely- doping level of the wide-gap material has to be higher than doping level of the narrow-gap one – can raise additionally its built-in voltage at the expanse of excess free *minority* carriers which appear in narrow-gap part of the junction. This fact and well known result of decreasing in built-in voltage of *p-n* junction when taking into account contribution of free *majority* carriers are in complete logical correspondence.

Fact that effect studied is particularly significant at large junction radius allows us to suggest that analogous effect has to take place also in planar electronic devices of analogous type.

Acknowledgement

This work was supported by the National Academy of Sciences of Ukraine.

Conclusion

Thus, correct solution of the Poisson equation with taking into account contribution of free (in given case - minority) carriers results in increasing in both thickness of space charge region and built-in potential of p^+-n heterojunction of the 1st type. If one remember that taking into account contribution of free majority carriers results in decreasing in both these parameters, then this fact looks as completely logical.

It is interesting that considered effect proves to be particularly significant in planar electronic devices of analogous type.

References

1. Costas, A., Florica, C., Preda, N., Kuncser, A., & Enculescu, I. (2020). Photodetecting properties of single CuO–ZnO core–shell nanowires with p–n radial heterojunction. *Scientific Reports*, 10. DOI: https://doi.org/10.1038/s41598-020-74963-4
2. Zhang, Y., & Liu, H. (2019). Nanowires for high-efficiency, low-cost solar photovoltaics. *Crystals, 9*(2), 87. DOI: https://doi.org/10.3390/cryst9020087
3. Goktas, N. I., Wilson, P., Ghukasyan, A., Wagner, D., McNamee, S., & LaPierre, R. R. (2018). Nanowires for energy: A review. *Applied Physics Reviews, 5*(4), 041305. DOI: https://doi.org/10.1063/1.5054842
4. Nami, M., Stricklin, I. E., DaVico, K. M., Mishkat-Ul-Masabih, S., Rishinaramangalam, A. K., Brueck, S. R. J., Brener, I., & Feezell, D. F. (2018). Carrier dynamics and electro-optical characterization of high-performance GaN/InGaN core-shell nanowire light-emitting diodes. *Scientific Reports, 8*(1), 501. DOI: https://doi.org/10.1038/s41598-017-18833-6
5. Hua, B., Motohisa, J., Kobayashi, Y., Hara, S., & Fukui, T. (2009). Single GaAs/GaAsP coaxial core-shell nanowire lasers. *Nano Lett, 9*(1), 112-116. DOI: https://doi.org/10.1021/nl802636b
6. Darbandi, A., Kavanagh, K. L., & Watkins, S. P. (2015). Lithography-free fabrication of core-shell GaAs nanowire tunnel diodes. *Nano Lett, 15*(8), 5408–5413. DOI: https://doi.org/10.1021/acs.nanolett.5b01795
7. Liborius, L., Bieniek, J., Possberg, A., Tegude, F. J., Prost, W., Poloczek, A., & Weimann, N. (2020). Tunneling-related leakage currents in coaxial GaAs/InGaP nanowire heterojunction bipolar transistors. *Physica Status Solidi (b), 258*(2), 2000395. DOI: https://doi.org/10.1002/pssb.202000395
8. Borblik, V. L. (2017). Concerning the depletion width of a radial p-n junction and its influence on electrical properties of the diode. *Semiconductor Physics, Quantum Electronics & Optoelectronics, 20*(2), 168-172. DOI: https://doi.org/10.15407/spqeo20.02.168

9. Borblik, V. L. (2018a). Electrostatics of nanowire radial p–n heterojunctions. *Journal of Electronic Materials*, 47, 4022-4027. DOI: https://doi.org/10.1007/s11664-018-6288-4
10. Borblik, V. L. (2018b). Comparative electrostatics of radial p-n heterojunctions with opposite sequences of the layers. *International Journal of Electrical and Electronic Science, 5*(2), 33-38. http://www.aascit.org/journal/archive2?journalId=915&paperId=6637
11. Borblik, V. L. (2024). Effects of non-reciprocity in multilayer semiconductor nanowires with radial subsequence of the layers. In O. Fesenko, L. Yatsenko, (Eds.), Nanooptics and Nanoelectronics, Nanobiotechnology, and Their Applications. (pp. 53-64). *Springer Proceedings in Physics*, Switzerland. DOI: https://doi.org/10.1007/978-3-031-67527-0_5
12. Sze, S. M., & Ng, K. K. (2006). Physics of Semiconductor Devices. (3rd edition). *John Wiley & Sons, Inc., Hoboken*, New Jersey. https://onlinelibrary.wiley.com/doi/book/10.1002/0470068329
13. Riben, A. R., & Feucht, D. L. (1966). nGe-pGaAs heterojunctions. *Solid-State Electronics, 9*(11-12), 1055-1065. DOI: https://doi.org/10.1016/0038-1101(66)90129-8
14. Donnelly, J. P., & Milnes, A. G. (1967). The capacitance of p-n heterojunctions including the effects of interface states. *IEEE Transactions on Electron Devices, 14*(2), 63-68. DOI: https://doi.org/10.1109/T-ED.1967.15900